Ferrimagnetic Behavior of Multiple Phases and Solvates of (*meso*-Tetrakis(4-chlorophenyl)porphinato)manganese(III) Tetracyanoethenide, $[MnTClPP]^+[TCNE]^{\bullet-}$. Enhancement of Magnetic Coupling by Thermal Annealing

Erik J. Brandon, Durrell K. Rittenberg, Atta M. Arif, and Joel S. Miller*

Contribution from the Department of Chemistry, University of Utah, Salt Lake City, Utah 84112-0850

Received December 4, 1997

(*meso*-Tetrakis(4-chlorophenyl)porphinato)manganese(III) tetracyanoethenide, [MnTClPP][TCNE], has been prepared and structurally characterized as the toluene and dichloromethane disolvates, and the magnetic and thermal properties of these solvates, as well as their corresponding desolvates, have been determined. The ditoluene solvate (**1**) has a triclinic unit cell: $P\bar{1}$, $a = 10.171(4)$ Å, $b = 10.189(3)$ Å, $c = 14.522$ (3) Å, $\alpha = 107.51(2)°$, $\beta = 85.58(2)°$, $\gamma = 111.51(3)°$, $Z = 1$. The bis(dichloromethane) solvate (**2**) belongs to the monoclinic unit cell: $P2_1/n$, $a = 9.894(2)$ Å, $b = 10.697(2)$ Å, $c = 23.560(5)$ Å, $\beta = 101.34(2)°$, $Z = 2$. The cation is typical with average Mn−N distances of 2.012 Å for both the toluene and dichloromethane solvates. The bonding distances for both planar anions are characteristic of $[TCNE]^{\bullet-}$. Both solvates have an uniform linear chain (1-D) coordination-polymer structure comprised of alternating cations and anions. Each $[TCNE]^{\bullet-}$ binds to two Mn^{III}'s in a *trans*-μ-*N*-σ-bound manner with Mn−N spacings of 2.267 (**1**) and 2.276 Å (**2**). The Mn−N−C angles are 167.2 and 143.1°, while intrachain Mn···Mn separations are 10.189 and 9.894 Å, and the dihedral angle between the MnN_4 and $[TCNE]^{\bullet-}$ mean planes are 86.8 and 52.4° for **1** and **2**, respectively. The ν_{CN} absorptions for the toluene and dichloromethane solvates occur at 2201 m and 2160 s cm^{-1} and 2195 m and 2138 s cm^{-1}, respectively. Upon thermolysis at 175 °C **1** desolvates to α-[MnTClPP][TCNE] with ν_{CN} absorptions at 2201 m and 2159 s cm^{-1}. In contrast, desolvation of **1** in refluxing *n*-octane leads to β-[MnTclPP][TCNE] with ν_{CN} absorptions at 2190 m and 2132 s cm^{-1}. Upon facile desolvation of **2** to form γ-[MnTClPP][TCNE] the nitrile absorptions remain essentially unchanged (2195 m and 2137 s cm^{-1}). For **1** and α the susceptibilities can be fit by the Curie−Weiss expression with $\Theta = -60$ K ($T > 210$ K) and −10 K ($T > 250$ K) and an effective Θ, Θ' of +13 ($50 < T < 120$ K) and 29 K ($60 < T < 160$ K), respectively. Θ is not observed for the **2** or the β- or γ-phase; however, Θ' for the **2** and the β- and γ-phases are 58, 92, and 86 K, respectively. The magnetic data are consistent with linear chain ferrimagnets comprised of antiferromagnetically coupled $S = 2$ Mn^{III} sites and $S = {}^1/_2$ $[TCNE]^{\bullet-}$ sites with the antiferromagnetic intrachain coupling, J/k_B (k_B = Boltzmann's constant) determined from fits to the Seiden expression, of −33, −160, −65, −267, and −265 K for the **1**, **2**, and α-, β-, and γ-phases, respectively. Hysteresis with a coercive field of 5.8 kOe is observed for **1** at 2 K. Metamagnetic behavior below 5 K is observed for the **1**, **2**, and β- and γ-phases with critical fields of 10, 27, 27, and 27 kOe, respectively. The ordering temperatures, T_c, determined from the maxima in the $\chi'(T)$ data taken at 10 Hz, are 8.8, 6.7, 11.1, 14.1, and 11.4 K for the phases **1**, α, β, **2**, and γ, respectively. Desolvation of **1** and **2** increases the magnetic disorder and the magnetic coupling.

Introduction

The preparation and characterization of molecule-based magnetic materials possessing spins on organic radicals is an area of increasing contemporary interdisciplinary research.[1,2] Magnetic ordering has been observed for several classes of materials that possess TCNE (tetracyanoethylene), *e.g.*, $[FeCp^*_2]^{\bullet+}[TCNE]^{\bullet-}$ (Cp^* = pentamethylcyclopentadienide) with a critical or ordering temperature, T_c, of 4.8 K,[3] $V(TCNE)_x$•

(1) Miller, J. S., Dougherty, D. A., Eds. Proceedings on the Conference on Ferromagnetic and High Spin Molecular Based Materials. *Mol. Cryst., Liq. Cryst.* **1989**, *176*. Kahn, O., Gatteschi, D., Miller, J. S., Palacio, F., Eds. Proceedings on the Conference on Molecular Magnetic Materials. *NATO ARW Mol. Magn. Mater.* **1991**, *E198*. Iwamura, H., Miller, J. S., Eds. Proceedings on the Conference on the Chemistry and Physics of Molecular Based Magnetic Materials. *Mol. Cryst., Liq. Cryst.* **1993**, *232/233*. Miller, J. S., Epstein, A. J., Eds. Proceedings on the Conference on Molecule-based Magnets. *Mol. Cryst., Liq. Cryst.* **1995**, *271−274*. Miller, J. S., Epstein, A. J., Eds. Proceedings on the Conference on Molecule-based Magnets. *Mol. Cryst., Liq. Cryst.* **1995**, *271−274*. Itoh, K., Miller, J. S., Takui, T., Guest Eds. Proceedings on the Conference on Molecular-Based Magnets. *Mol. Cryst., Liq. Cryst.* **1997**, *305−306*. Turnbull, M. M.; Sugimoto, T.; Thompson, L. K. *ACS Symp. Ser.* **1996**, *644*.

(2) Reviews: (a) Buchachenko, A. L. *Russ. Chem. Rev.* **1990**, *59*, 307; *Usp. Khim.* **1990**, *59*, 529. Kahn, O. *Struct. Bonding* **1987**, *68*, 89. Kahn, O. *Molecular Magnetism*; VCH Publishers, Inc.: New York, 1993. (b) Caneschi, A.; Gatteschi, D.; Sessoli, R.; Rey, P. *Acc. Chem. Res.* **1989**, *22*, 392. Gatteschi, D. *Adv. Mater.* **1994**, *6*, 635. (c) Miller, J. S.; Epstein, A. J.; Reiff, W. M. *Acc. Chem. Res.* **1988**, *21*, 114. Miller, J. S.; Epstein, A. J.; Reiff, W. M. *Science* **1988**, *240*, 40. Miller, J. S.; Epstein, A. J.; Reiff, W. M. *Chem. Rev.* **1988**, *88*, 201. Miller, J. S.; Epstein, A. J. In *New Aspects of Organic Chemistry*; Yoshida, Z., Shiba, T., Ohsiro, Y., Eds.; VCH Publishers: New York, 1989; Vol. 237. Miller, J. S.; Epstein, A. J. *Angew. Chem., Int. Ed. Engl.* **1994**, *33*, 385; *Angew. Chem.* **1994**, *106*, 399. Miller, J. S.; Epstein, A. J. *Adv. Chem. Ser.* **1995**, *No. 245*, 161.

(3) Miller, J. S.; Calabrese, J. C.; Dixon, D. A.; Epstein, A. J.; Bigelow, R. W.; Zhang, J. H.; Reiff, W. M. *J. Am. Chem. Soc.* **1987**, *109*, 769. Miller, J. S.; Calabrese, J. C.; Epstein, A. J.; Bigelow, R. W.; Zhang, J. H.; Reiff, W. M. *J. Chem. Soc., Chem. Commun.* **1986**, 1026. Chittipeddi, S.; Cromack, K. R.; Miller, J. S.; Epstein, A. J. *Phys. Rev. Lett.* **1987**, *22*, 2695.

S0020-1669(97)01521-8 CCC: $15.00
Published on Web 06/11/1998

y(solvent) ($T_c \sim 400$ K),[4] and $[MnTPP]^+[TCNE]^{\bullet-}\cdot 2PhMe$ (TPP = *meso*-tetraphenylporphinato)[5] ($T_c = 13$ K). Current research focuses on establishing relationships between structure and magnetic phenomena, particularly in the correlation of dimensionality, connectivity, and the critical temperature of the material.[1,2]

Due to the ease of modifying the porphyrin structure, as well as inclusion of differing solvate chlaterates[6] to alter the 3-D packing motifs, we are studying modified MnTPP systems in several solvents to identify changes in the inter- and intrachain couplings as well as ordering temperatures to determine a structure-function relationship. Herein we report the structure, magnetic properties, and thermal behavior of (*meso*-tetrakis(4-chlorophenyl)porphinato)manganese(III) tetracyanoethenide, $[MnTClPP]^+[TCNE]^{\bullet-}$ prepared from the redox polymerization of MnTClPP and TCNE.

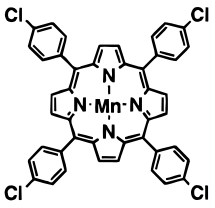

MnTClPP

Experimental Section

Synthesis. All manipulations involving $[TCNE]^{\bullet-}$ were carried out under an atmosphere of nitrogen using standard Schlenk techniques or in a Vacuum Atmospheres DriLab. Solvents used for the preparation of the $[TCNE]^{\bullet-}$ salts were predried and distilled from appropriate drying agents. H_2TClPP was prepared by a literature method.[7a] $[Mn^{III}TClPP][OAc]$ was prepared from H_2TClPP and $Mn(OAc)_2\cdot 4H_2O$; the $Mn(OAc)_2\cdot 4H_2O$ was predissolved in *N*,*N*-dimethylformamide and filtered before addition to the free-base porphyrin, to remove paramagnetic impurities. The $[Mn^{III}TClPP]^+$ salt was subsequently reduced to $Mn^{II}TClPP$ as the pyridine adduct, $Mn^{II}TClPP(py)$, by $NaBH_4$ utilizing a literature method.[7b] TCNE was resublimed prior to use.

[MnTClPP][TCNE]·*x*PhMe (1) was prepared by the reaction of filtered solutions of $Mn^{II}TClPP(py)$ (125.7 g, 0.1421 mmol) dissolved in 30 mL of toluene and TCNE (0.0279 g, 0.218 mmol) dissolved in 20 mL of toluene. The two solutions were mixed and allowed to stand at room temperature for 4 days in an inert-atmosphere glovebox. The resulting dark-green precipitate was filtered off and washed three times with 10 mL portions of fresh, dry toluene and dried *in vacuo* for 1.5 h at room temperature [yield: 117.3 mg (74%)]. IR (Nujol; cm^{-1}): ν_{CN} 2201 m, 2160 s. Anal. Calcd for $[MnTClPP]^+[TCNE]^{\bullet-}\cdot{}^4/_3PhMe$ ($C_{61.69}H_{37.39}Cl_4MnN_8$): C, 68.14; H, 3.46; N, 10.31. Found: C, 67.98; H, 3.54; N, 10.02.

Crystals suitable for X-ray diffraction studies were obtained by a modification of the above procedure in which a 1:1 dichloromethane/toluene solution (30 mL) containing $Mn^{II}TClPP(py)$ (47.6 mg, 0.054 mmol) was mixed with a 20 mL toluene solution of TCNE (11.7 mg, 0.0913 mmol). Upon standing in an vibration-dampened inert-atmosphere DriLab for 12 days, long, thin platelike crystals were harvested from the mother liquor.

α-[MnTClPP][TCNE]. A glass vial containing freshly prepared $[MnTClPP][TCNE]\cdot x$PhMe (ca. 75 mg) was heated in a tube furnace under dynamic vacuum at 175 °C for 3 h. Anal. Calcd for $C_{50}H_{24}Cl_4MnN_8$ (no toluene): C, 64.33; H, 2.59; N, 12.00. Found: C, 64.19; H, 2.63; N, 11.82. IR (Nujol; cm^{-1}): ν_{CN} 2201 m, 2159 s.

β-[MnTClPP][TCNE]. In an inert-atmosphere glovebox a Schlenk flask was charged with $[MnTClPP][TCNE]\cdot 2PhMe$ (183.0 mg, 0.1637 mmol) and 30 mL of dry *n*-octane. The resulting suspension was heated to reflux (~126 °C) under nitrogen for 30 min with magnetic stirring and then cooled to room temperature. The resultant black solid was collected by vacuum filtration on a glass-frit funnel, yielding 127.7 mg (84%) of the β-phase. Anal. Calcd for $C_{50}H_{24}Cl_4MnN_8$ (no toluene): C, 64.33; H, 2.59; N, 12.00. Found: C, 64.04; H, 2.47; N, 11.87. IR (Nujol; cm^{-1}): ν_{CN} 2190 m, 2132 s.

[MnTClPP][TCNE]·2CH$_2$Cl$_2$ (2). Filtered solutions of $Mn^{II}TClPP(py)$ (53.1 mg, 0.0600 mmol) and TCNE (7.8 mg, 0.0609 mmol) (20 mL each) were mixed and stirred under nitrogen at room temperature for 4 h. The mixture was then layered with 40 mL of hexanes and let to stand for 3 days in an inert-atmosphere glovebox. The resulting precipitate was then collected by vacuum filtration. Single crystals suitable for X-ray diffraction were isolated by slow diffusion of $MnTClPP(py)$ (100.3 mg, 0.1343 mmol) dissolved in 35 mL of dichloromethane and TCNE (17.3 mg, 0.135 mmol) also dissolved in 35 mL of dichloromethane and both solutions filtered. An "H-tube" crystal-growing apparatus comprised of two chambers separated by a medium glass frit was charged on either side with these solutions and allowed to stand in a vibration-dampened inert atmosphere DriLab for 9 days. Blocklike crystals of the product were isolated and allowed to sit under the mother liquor until transferred to the diffractometer, at which time they were covered with oil and immediately cooled to −80 °C under a stream of cold nitrogen. The crystals lose solvent after several seconds in air/nitrogen and quickly turn into a powder. As **2** readily lost solvent under ambient conditions, samples for infrared spectroscopy were mulled in mineral oil with a small portion of the mother liquor immediately after isolation from the reaction solution; quantitative thermogravimetric analysis could not be performed due to this rapid desolvation. Magnetic studies were made in an airtight holder. IR (Nujol; cm^{-1}): ν_{CN} 2195 m, 2138 s.

γ-[MnTClPP][TCNE]. The desolvated, γ-phase was obtained by drying the $[MnTClPP][TCNE]\cdot 2CH_2Cl_2$ sample *in vacuo* for 1 h, yielding 39.3 mg (70%) of shiny black microcrystals. IR (Nujol; cm^{-1}): ν_{CN} 2195 m, 2137 s. Anal. Calcd for $C_{50}H_{24}Cl_4MnN_8$ (no CH_2Cl_2): C, 64.33; H, 2.59; N, 12.00. Found: C, 64.05; H, 2.57; N, 11.86.

Physical Methods. The 2−300 K dc magnetic susceptibility was determined on the equivalent of a Quantum Design MPMS-5XL 5 T SQUID (sensitivity = 10^{-8} emu or 10^{-12} emu/Oe at 1 T) magnetometer with an ultra-low-field (~0.005 Oe) option, an ac option enabling the study of the ac magnetic susceptibility (χ' and χ'') in the range of 10−1000 Hz, a reciprocating sample measurement system, and continuous low-temperature control with enhanced thermometry features. The 2−40 K ac magnetic susceptibility was also determined on a Quantum Design PPMS-9 ac/dc magnetometer. Samples were loaded in an airtight Delrin holder and packed with oven-dried quartz wool (to prevent movement of the sample in the holder). For isofield dc measurements, the samples were zero-field cooled (following oscillation of the dc field), and data were collected upon warming. For ac measurements, remanent fluxes were minimized by oscillation of the dc field, with the sample cooled in zero applied field with data then taken upon warming. In addition to correcting for the diamagnetic contribution from the sample holder, core diamagnetic corrections of -558×10^{-6}, -66×10^{-6}, and -47×10^{-6} emu/mol were used for [MnTClPP][TCNE], PhMe, and CH_2Cl_2, respectively. The thermal properties were studied on a TA Instruments model 2050 thermal gravimetric analyzer (TGA) (ambient to 1000 °C) located in a Vacuum

(4) Miller, J. S.; Yee, G. T.; Manriquez, J. M.; Epstein, A. J. In *Proceedings of Nobel Symposium #NS-81 Conjugated Polymers and Related Materials: The Interconnection of Chemical and Electronic Structure*; Oxford University Press: New York, 1993; p 461. *Chim. Ind.* **1992**, *74*, 845. Epstein, A. J.; Miller, J. S. In *Proceedings of Nobel Sympsoium #NS-81 Conjugated Polymers and Related Materials: The Interconnection of Chemical and Electronic Structure*; Oxford University Press: New York, **1992**; p 475. *Chim. Ind.* **1993**, *75*, 185.

(5) Miller, J. S.; Calabrese, J. C.; McLean, R. S.; Epstein, A. J. *Adv. Mater.* **1992**, *4*, 498.

(6) Goldberg, I.; Krupitsky, H.; Stein, Z.; Hsiou, Y.; Strouse, C. E. *Supramolecular Chem.* **1995**, *4*, 203. Krupitsky, H.; Stein, Z.; Goldberg, I. J. *Inclusion Phenom. Mol. Recognit.* **1995**, *20*, 211. Goldberg, I. *Mol. Cryst. Liq. Cryst.* **1996**, *278*, 767. Byrn, M. P.; Curtis, C. J.; Hsiou, Y.; Kahn, S. I.; Sawin, P. A.; Tendick, S. K.; Terzis, A.; Strouse, C. E. *J. Am. Chem. Soc.* **1993**, *115*, 9480.

(7) Jones, R. D.; Summerville, D. A.; Basolo, F. *J. Am. Chem. Soc.* **1978**, *100*, 4416. (a) Milgrom, L. R. *Tetrahedron* **1983**, *39*, 3895. (b) Ozawa, T.; Hanaji, A. *Inorg. Chim. Acta* **1987**, *130*, 231.

Table 1. Crystallographic Details

	[Mn^{III}TClPP][TCNE]·2MePh		
chem formula	$C_{64}H_{40}Cl_4MnN_8$	formula mass, Da	1117.78
a	10.171(4) Å	space group	$P\bar{1}$ (No. 2)
b	10.189(3) Å	*T*	−80 °C
c	14.522(3) Å	λ	0.710 73 Å
α	107.51(2)°	ρ_{calcd}	1.391 g cm^{-3}
β	85.58(2)°	μ	0.0498 cm^{-1}
γ	111.51(3)°	$R1^a$	0.0426
V	1334.4(7) Å^3	w$R2^b$ =	0.0831
Z	1		
	[Mn^{III}TClPP][TCNE]·2CH_2Cl_2		
chem formula	$C_{52}H_{28}Cl_8MnN_8$	formula mass, Da	1103.42
a	9.894 (2) Å	space group	$P2_1/n$ (No. 14)
b	10.697 (2) Å	*T*	−80 °C
c	23.560 (5) Å	λ	0.710 73 Å
β	101.34 (2)°	ρ_{calcd}	1.499 g cm^{-3}
V	2444.6 (8) Å^3	μ	0.0754 cm^{-1}
Z	2	$R1^a$	0.0411
		w$R2^b$ =	0.1034

^{a} $\sum(|F_o| - |F_c|)/\sum|F_o|$. ^{b} $\{\sum w[F_o^2 - F_c^2]^2/\sum w[F_o^2]^2\}^{1/2}$.

Atmospheres DriLab under nitrogen to study air- and moisture-sensitive samples. Samples were placed in an aluminum pan and heated at 20 °C/min under a continuous 10 mL/min nitrogen flow. Differential scanning calorimetry (DSC) was performed on a TA Instruments model 2910 DSC equipped with a LNCA liquid nitrogen cooling accessory enabling operation between −150 to 550 °C using a modulated DSC cell or up to 750 °C using a regular DSC cell. Data were taken on both open and hermetically sealed aluminum DSC pans. Infrared spectra (625−4000 cm^{-1}) were obtained on a Perkin-Elmer 783 or a Mattson Galaxy Series FTIR 3000 spectrophotometer. Elemental analyses were performed on a Perkin-Elmer model 2400 elemental analyzer and by Atlantic Microlabs, Norcross, GA. Powder XRD patterns were obtained on a Rigaku model 1GC2 Miniflex diffractometer over the range 2−35° 2θ using Cu Kα radiation. Samples were prepared in an inert-atmosphere glovebox, mixed with a small amount of silicon powder standard, and affixed to a glass slide with vacuum grease. The slide was then placed in an airtight holder (fitted with a Mylar window) and mounted onto the diffractometer. Measurements were made every 0.05° with a collection time of 30 s. The data were corrected relative to the first Si peak.

X-ray Structure Determination. Cell constants and an orientation matrix for the data collection were obtained by the standard methods from 25 reflections at −80 °C on a CAD4 diffractometer. Systematic absences and subsequent least-squares refinement were used to determine the space groups. During data collection the intensities of several representative reflections were measured as a check on crystal stability. There was no loss of intensity during data collection. Equivalent reflections were merged, and only those for which $I_o > 2\sigma(I)$ were included in the refinement, where $\sigma(F_o)^2$ is the standard deviation based on counting statistics. The weighing scheme used was $[\sigma^2(F_o^2)]^{-1}$. SHELX-93 was used for the refinement based on the Patterson method.[8a] Non-hydrogen atoms were refined anisotropically. Further refinement/analysis to locate disordered [TCNE]$^{\bullet-}$ was performed through examination of electron density difference maps as previously described. Data were also corrected for Lorentz and polarization factors. Empirical absorption corrections were applied. Crystallographic details are summarized in Table 1, and tables of the atomic coordinates, anisotropic thermal parameters, and bond angles are provided as Supporting Information. The hydrogen atoms were included using the riding model where the H-atom coordinates are reidealized before each refinement cycle and "ride" on the atoms to which it is attached. Disorder in the [TCNE]$^{\bullet-}$ and solvent was not observed.[8b]

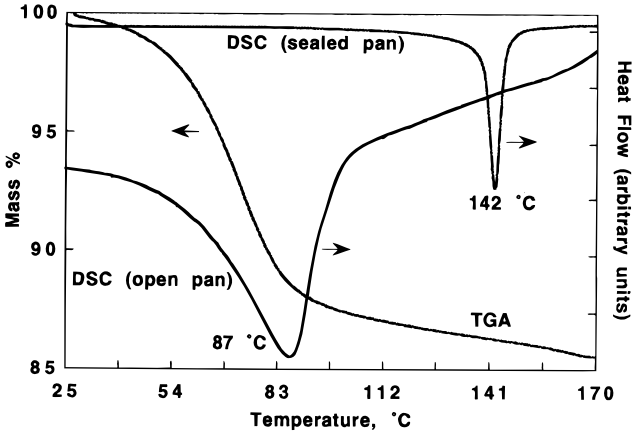

Figure 1. DSC and TGA as a function of temperature for β-[MnTClPP][TCNE]. Note the offset of the baseline for data measured in an open pan, due to the changing of the specific heat of the sample as a result of desolvation.

Results and Discussion

Synthesis and Characterization. [MnTClPP][TCNE]·2PhMe (**1**) may be isolated from toluene or toluene/dichloromethane mixtures; however, when pure dichloromethane is used, [MnTClPP][TCNE]·2CH_2Cl_2 (**2**) is obtained. The $\nu_{C\equiv N}$ absorptions at 2201 m and 2160 s cm^{-1} and 2195 m and 2138 s cm^{-1} for the toluene and dichloromethane solvates, respectively, confirm the presence of [TCNE]$^{\bullet-}$ and are inconsistent with [TCNE]^n [n = 0 (2259 s, 2221 m cm^{-1}), 2− (2104 s, 2069 s cm^{-1})].[9] This range of energies is consistent with the 2192 m and 2147 s cm^{-1} values reported for [MnTPP][TCNE]·2PhMe, **3**,[5] and the 2195 m and 2133 s cm^{-1} values reported for [MnTP′P][TCNE]·2PhMe [H_2TP′P = tetrakis(3,5-di-*tert*-butyl-4-hydroxyphenyl)porphyrin], **4**.[10]

A shift in the observed ν_{CN} absorptions does not occur upon heating of **1** *in vacuo* or under a nitrogen atmosphere, both of which result in desolvation only (designated as the α-phase). This may be monitored by thermogravimetric analysis (TGA) and differential scanning calorimetry (DSC). The TGA of **1** confirms the presence of two toluenes of solvation per unit cell which are lost predominately below ∼73 °C (Figure 1), while the DSC of **1** indicates an irreversible endotherm at 142 °C when studied in a closed pan, which shifts to 87 °C when studied in an open pan. Upon heating of a sample mulled in Nujol above 110 °C, however, the ν_{CN} absorptions at 2201 m and 2160 s cm^{-1} irreversibly disappear while new absorptions at 2190 m and 2132 s cm^{-1} appear.[11a] Bulk samples of the material exhibiting the shifted reduced ν_{CN} absorptions could be isolated upon thermal treatment of the ditoluene solvate in an *n*-octane reflux (designated the β-phase).[11b] Due to rapid desolvation of **2**, detailed physical measurements were not possible, except for the magnetic studies due to the availability of an airtight holder. Total solvent loss from **2** forms the γ-phase without altering the frequencies of the nitrile absorptions. Powder X-ray diffraction reveals that all three desolvated materials exhibit unique diffraction patterns; hence, three distinct desolvated phases may be isolated. Since the ν_{CN} absorptions are sensitive to the local bonding, desolvation without significant changes in the frequencies is assumed to proceed with maintenance of the intrachain but not necessarily the interchain structure.

(8) (a) Sheldrick, G. M. Manuscript in preparation. (b) Using the program CHAIN [Sack, J. S. *J. Mol. Graph.* **1988**, *6*, 224] on a graphics workstation evidence for disorder of the cation, anion, and solvent was sought without success: Burkhart, B. M. Private communication.

(9) Dixon, D. A.; Miller, J. S. *J. Am. Chem. Soc.* **1987**, *109*, 3656.

(10) Böhm, A.; Vazquez, C.; McLean, R. S.; Calabrese, J. C.; Kalm, S. E.; Manson, J. L.; Epstein, A. J.; Miller, J. S. *Inorg. Chem.* **1996**, *35*, 3083.

Despite the lack of consistent rate data,[11b] several conclusions concerning the **1** to β-phase transformation can be made. As TGA/DSC indicates desolvation of the solvate (in a nitrogen atmosphere) occurs primarily between ca. 75 and 85 °C and variable-temperature IR data indicate transformation to the β-phase (in mineral oil mulls) occurs at significant rates above 110 °C, it is presumed that solvent loss precedes the probable structural rearrangement. Also, as the ν_{CN} absorbances are particularly sensitive to changes in the intrachain bonding parameters, a significant change in the intrachain structure occurs as evidenced by the shift of the 2162 cm^{-1} absorbance to 2133 cm^{-1}. Initial correlations between the MnNC bond angle and parameters that correlate to magnetic coupling indicate that this corresponds to a "collapse" of the chain structure, in which the Mn−N−C bond angle decreases significantly.[13]

Structure. Structure determinations of both **1** and **2** reveal one-half of an ordered $[Mn^{III}TClPP]^+[TCNE]^{\bullet-}$ where both the cation and anion each reside on a center of symmetry, Figure 2. The average Mn^{III}−N(ring) distances of 2.012 Å and the remaining bond distances and angles are typical of Mn^{III}-(porphyrins).[5,10,14] $[TCNE]^{\bullet-}$ is planar with a 0.0° twist for both **1** and **2**; this is in contrast to the 1.9° twist observed for **3**.[5]

The solid state motifs of both **1** and **2** are comprised of 1-D $\cdots D^+A^{\bullet-}D^+A^{\bullet-}\cdots$ polymer chains (D = MnTClPP; A = TCNE), where $[TCNE]^{\bullet-}$ is *trans*-μ-*N*-σ-bound to Mn^{III}'s (Figures 3−6; Table 2) with Mn−N distances of 2.267(3) Å and 2.276(2) Å, respectively, which are shorter than that observed in **3**[5] [2.306(4) Å] and **4**[10] [2.299(10) Å]. The Mn−N−C angles differ significantly being 167.2(3)° for **1** and 143.1(2)° for **2** and 147.6(4) and 129.0(1)° reported for **3**[5] and **4**,[10] respectively. The dihedral angles between the mean planes of $[MnTClPP]^+$ and $[TCNE]^{\bullet-}$ also significantly differ and are 86.8, 52.4, 55.4,[5] and 30.4° [10] for **1**−**4**, respectively.

The 10.189 Å (**1**) and 9.894 Å (**2**) intrachain Mn···Mn separations fall in a similar range for **3** (10.116 Å)[5] and **4** (8.587 Å).[10] The key intra- and interchain Mn···Mn separations for **1**−**4** are listed in Table 2 and depicted for **1** and **2** in Figures 3−6. In contrast to **3** and **4** which lack sub-van der Waals interchain interactions, [MnTClPP][TCNE]·2PhMe has close contacts between Cl(1) and $[TCNE]^{\bullet-}$ C(1)′ of 3.371 Å.

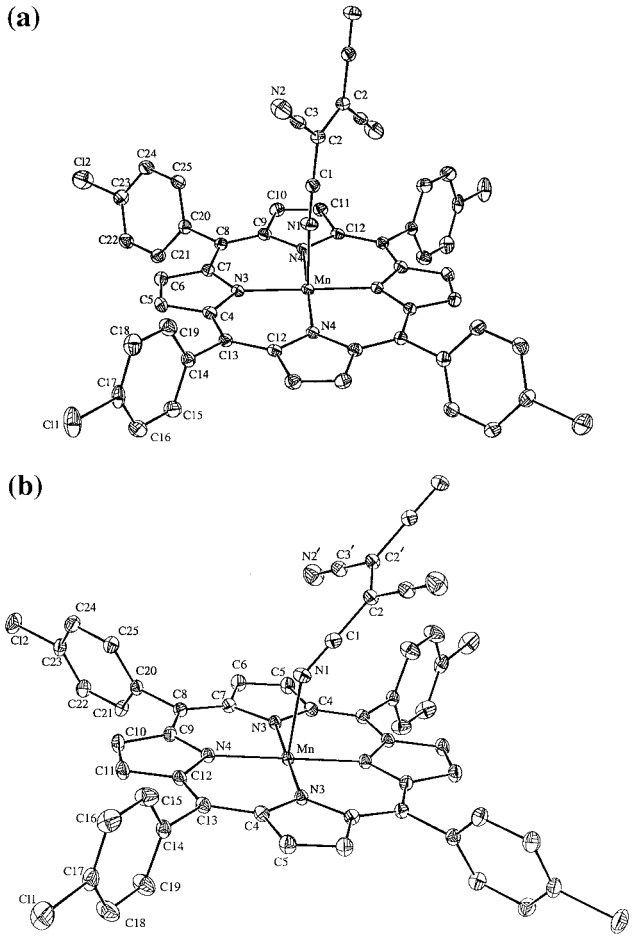

Figure 2. Labeling diagram and ORTEP (30% probability level) diagram for (a) for [MnTClPP][TCNE]·2PhMe (**1**) and (b) [MnTClPP]-[TCNE]·$2CH_2Cl_2$ (**2**).

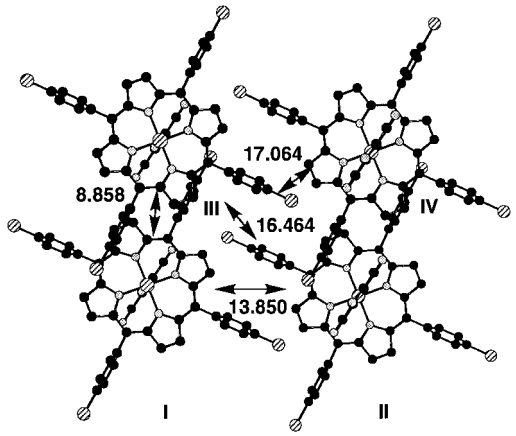

Figure 3. View down the crystallographic *b* (chain) axis for [MnTClPP]-[TCNE]·2PhMe (**1**).

Complex **2** is unusual with respect to the [MnTPP][TCNE]·2PhMe family due to the arrangement of the nearest-neighbor parallel chains. All parallel chains in **1**, **3**,[5] and **4**[10] have the same orientation as do the **I**−**II** and **III**−**III**′ chains for **2**, Figure 6; however, as a consequence of the crystal symmetry, chains **I**−**III** (and **II**−**III**) have differing orientations as noted in Figure 6 which may lead to differing magnetic behaviors particularly in terms of interchain coupling.

Magnetic Behavior. The 2−300 K reciprocal corrected magnetic susceptibility (χ^{-1}) and effective moment, μ_{eff} [$\equiv(8\chi T)^{1/2}$], of **1**, **2**, α, β, and γ are presented in Figure 7 and

(11) (a) Similar behavior is observed when the materials are crystallized from benzene. (b) The thermally induced **1** to β transformation was monitored by variable-temperature IR (VTIR) spectroscopy. Samples prepared as mineral oil mulls between NaCl plates were heated to a constant temperature (≤200 °C) in an high-temperature cell, and the disappearance of the 2162 cm^{-1} absorbance was monitored as a function of time at several temperatures. Since attainment of the desired temperature was not instantaneous, a 2-min lagtime was used, as the sample was placed into the preheated cell holder at the desired temperature and data were taken after 2 min lapsed. Data were taken until *ca.* 90% conversion was achieved. The data were fit to the Avrami equation which has been successfully applied to several molecular solid-state transformations.[12] Although many of the samples displayed Arrenhius type behavior, some exhibited incomplete or no conversion. This was ascribed to differences in crystallinity, solvation, or sample preparation. Also, the specific role of solvent (*n*-octane or, in this case, mineral oil) is unclear. We are continuing further work aimed at understanding this transformation and the kinetic data.

(12) Rao, C. N. R.; Rao, K. J. *Phase Transitions in Solids*; McGraw-Hill: San Franscisco, CA, 1978. Bym, S. R. *Solid-State Chemistry of Drugs*; Academic: New York, 1982; pp 59−75.

(13) Brandon, E. J.; Kollmar, C.; Miller, J. S. *J. Am. Chem. Soc.* **1998**, *120*, 1822.

(14) Landrum, J. T.; Hatano, K.; Scheidt, W. R.; Reed, C. A. *J. Am. Chem. Soc.* **1980**, *102*, 6729. Hill, C. L.; Williamson, M. M. *Inorg. Chem.* **1985**, *24*, 2834, 3024. Fleischer, E. B. *Acc. Chem. Res.* **1970**, *3*, 105. Scheidt, W. R.; Reed, C. A. *Chem. Rev.* **1981**, *81*, 543. Turner, P.; Gunter, M. J.; Hambley, T. W.; White, A. H.; Skelton, B. W. *Inorg. Chem.* **1992**, *31*, 2297. Sugiura, K.-i.; Arif, A.; Schweizer, J.; Öhrstrom, L.; Epstein, A. J.; Miller, J. S. *Chem. Eur. J.* **1997**, *3*, 138.

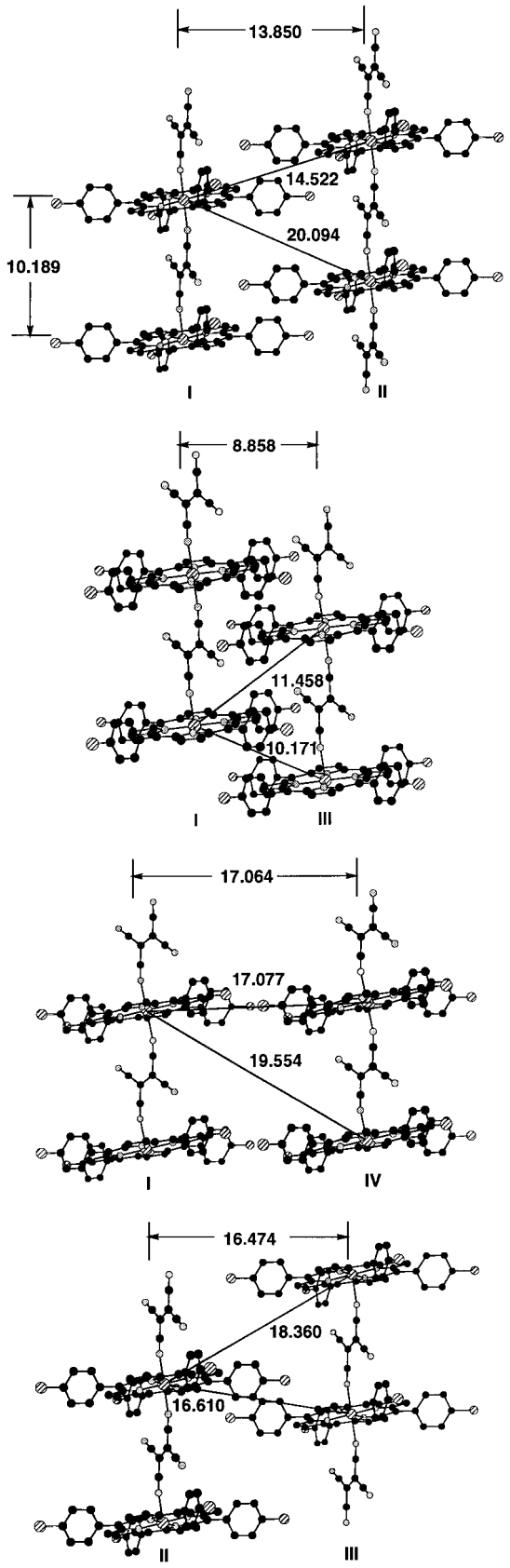

Figure 4. View of intra- and interchain interaction among the unique chains **I**, **II**, **III**, and **IV** as depicted in Figure 3 for [MnTClPP][TCNE]·2PhMe. Note the $[TCNE]^{\bullet-}$ *trans*-μ-*N*-σ-bonding to $[MnTClPP]^{+}$ and the uniform chains. The hydrogen atoms and toluenes of solvation are omitted for clarity.

are summarized in Table 3. The room-temperature effective moments range from 4.69 to 5.40 μ_B, which are close to the

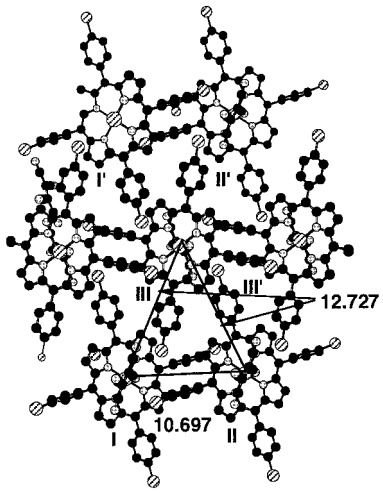

Figure 5. View down the crystallographic *b* (chain) axis for [MnTClPP][TCNE]·$2CH_2Cl_2$ (**2**).

calculated spin-only value of 5.20 μ_B for a system comprised of noninteracting $S = 2$ and $S = {}^1/_2$ spin sites and are typical for this class of materials.[5,10] Values below 5.20 μ_B result from antiferromagnetic coupling still present at room temperature, while the genesis of the 5.40 μ_B value is unknown but may arise from uncertainty in the molecular weight (related to the specific degree of solvation). The susceptibility for all compounds can be fit by the Curie−Weiss expression, $\chi \propto 1/(T - \Theta)$. For **1** and α two linear regions can be fit to this expression. For **1** Θ is −60 K for data above 180 K, while Θ′ is 13 K for data taken between 50 and 120 K. The latter, ferromagnetic 13 K value is not the intrinsic Θ value but reflects a second, lower temperature linear region for $\chi^{-1}(T)$ and hence is termed an effective Θ, Θ′.[10] For α Θ is −10 K for $T > 250$ K and Θ′ is 29 K for data taken between 60 and 160 K. **2**, β, and γ do not have determinable Θ values as data must be acquired at a higher temperature. Θ′ values of 58, 92, and 86 K, for **2**, β, and γ, respectively, are observed and reflect stronger magnetic couplings. Hence, as reflected in the identical ν_{CN} absorptions, thermal desolvation of both **1** and **2** forms phases (α and γ) that nominally maintain the intrachain interactions, but solvent loss enables the parallel chains to get closer together leading to stronger interchain interactions as reflected in Θ′ increasing from 13 to 29 K for **1** and 58 to 86 K for **2**. These interactions are stronger for **2**, β, and γ as the expected larger Θ cannot be observed, although the expected concomitant larger Θ′′s are observed.[15] In contrast, heating **1** in *n*-octane likely alters the intrachain as well as the interchain structures. This is evidenced by the reduction of the ν_{CN} absorption frequencies and an increase in Θ′ for β with respect to α. These Θ′ values for the solvates, **1** and **2**, are significantly lower than the 61 and 90 K reported for uniformly-chained **3**[5] and **4**,[10] respectively, suggesting weaker intrachain interactions. Thermolysis of **1** and desolvation of **2** leads to stronger magnetically coupled phases, and the 92 K Θ′ value for β-[MnTClPP][TCNE] is the largest Θ value reported to date for the $[Mn(por)]^{+}$ family of magnets.[5,10,14] The greater Θ′ value for **2** with respect to **1** is consistent with the an inverse correlation between Θ′ and the dihedral angle between the mean MnN_4 and $[TCNE]^{\bullet-}$ mean planes. Both the dihedral angle and Θ′ are comparable for **2** (52.4°, 58 K) and **3** (55.4°, 61 K), while the **4** has a substantially reduced dihedral angle (30.4°) and enhanced Θ′ (90 K). In

(15) Next-nearest-neighbor intrachain interactions may also contribute to the ferromagnetic coupling.

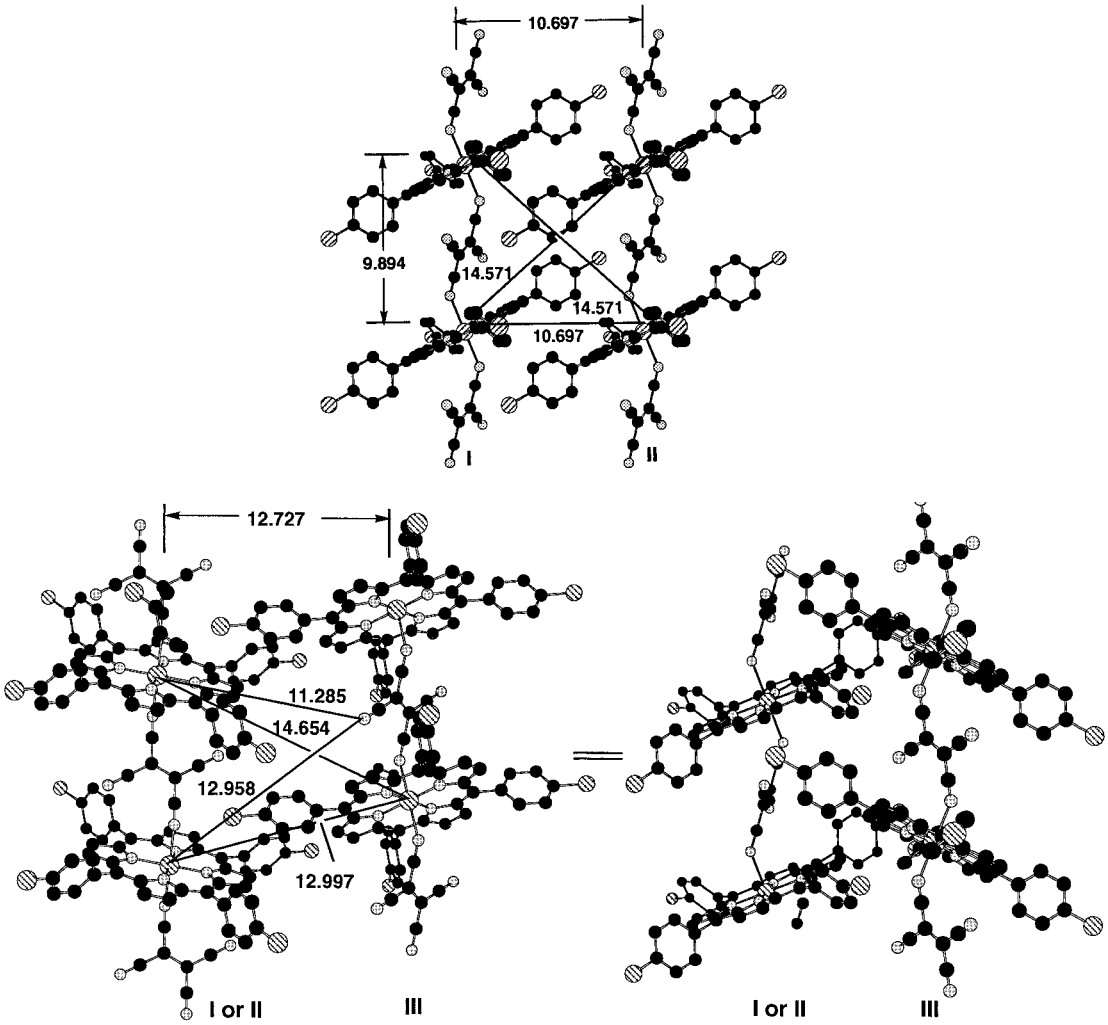

Figure 6. View of intra- and interchain interaction among the unique chains **I**, **II**, and **III** as depicted in Figure 5 for $[MnTClPP][TCNE]\cdot 2CH_2Cl_2$. Note the $[TCNE]^{\bullet-}$ *trans-μ-N-σ*-bonding to $[MnTClPP]^+$ as well as the herringbone arrangement of the chains. The hydrogen atoms and toluenes of solvation are omitted for clarity.

Table 2. Comparison of the Inter- and Intrachain Mn···Mn and Mn···N Distances and Mn−N−C Angles for **1**−**4**

cation (solvent)	Mn···Mn intrachain, Å	Mn···Mn interchain, Å	$Mn\cdots N_{TCNE}$ intrachain, Å	interchain separatns, Å	∠Mn−N−C_{TCNE}, deg	∠MnN_4−TCNE, dihedral angle, deg
$[MnTClPP]^+$	10.189	10.171	2.267	8.858	167.2	86.8
(PhMe), **1**		11.458		13.850		
		14.522		16.474		
		16.610				
$[MnTClPP]^+$	9.894	10.697	2.276	10.697	143.1	52.4
(CH_2Cl_2), **2**		12.958		12.727		
$[MnTPP]^+$	10.116	11.006	2.306	10.201	147.6	55.4
(PhMe), **3**		11.829		13.139		
		13.269		13.630		
		13.838				
$[MnTP'P]^+$	8.587	14.756	2.299	14.665	129.0	30.4
(PhMe), **4**		16.233		17.071		
		17.573		17.275		

contrast **1** has a larger dihedral angle (86.6°) and a reduced Θ′ (13 K). This correlation is the focus of an independent study.[13]

The ferrimagnetic nature of this class of magnets is evident from the minimum, T_{min}, albeit shallow, in the $\mu(T)$ and $\chi T(T)$ data,[16] Figures 7 and 8, which range from 110 K (**1**) to above room temperature for β and γ, Table 3. Due to the shallowness of the minimum as well as slight variations which occur between samples, the accuracy of T_{min} is estimated at ±20 K. Like Θ′, T_{min} correlates monotonically with magnetic coupling, Table 3. T_{min} is model independent but cannot be observed for strongly coupled systems as it occurs at temperatures exceeding the experimental range.

The data, as $\chi T(T)$, were modeled using a least-squares fit to an analytical expression for isolated chains comprised of

(16) Coronado, E.; Drillon, M.; Georges, R. In *Research Frontiers in Magnetochemistry*; O'Connor, C. J., Ed.; World Scientific: Singapore, 1993; p 26. Beltran, D.; Drillon, M.; Coronado, E.; Georges, R. *Stud. Inorg. Chem.* **1983**, *3*, 589. Drillon, M.; Coronado, E.; Beltran, D.; Georges, R. *Chem. Phys.* **1983**, *79*, 449. Verdaguer, M.; Julve, M.; Michalowicz, A.; Kahn, O. *Inorg. Chem.* **1983**, *22*, 2624. Drillon, M.; Gianduzzo, J. C.; Georges, R. *Phys. Lett. A* **1983**, *96A*, 413.

Table 3. Summary of the ν_{CN} Absorptions and Magnetic Properties of **3**, **4**, and [MnTClPP][TCNE]·2S (S = PhMe, CH_2Cl_2) and α-, *β*-, and *γ*-[MnTClPP][TCNE]

compd	ν_{CN}, cm^{-1}	Θ, K	Θ′, K	M_s,[a] emuOe/mol	μ_{eff}, μ_B	$\chi'(T_c)$,[b] K	χ'',[b] K	T_{min}, K	H_c,[c] kOe	J/k_B,[d] K	J/k_B,[e] K	ϕ
[MnTPP][TCNE]· 2PhMe, **3**[5,21]	2192 m 2147 s	*f*	61	17 000	5.12	14	13	*f*	24	*g*	*f*	0.18
[MnTClPP][TCNE]· 2PhMe, **1**	2201 m 2160 s	−60	13	11 000	4.69	8.8	6.4	110	10	−33	−26	0.017
α-[MnTClPP][TCNE]	2201 m 2159 s	−10	29	18 500	4.89	6.7	5.8	192		−65	−46	0.15
β-[MnTClPP][TCNE]	2190 m 2132 s	*f*	92	15 800	5.05	11.1	9.6	800[d]	27	−267	−190	0.14
[MnTClPP][TCNE]· $2CH_2Cl_2$, **2**	2195 m 2138 s	*f*	58	14 000	5.10	14.1	8.0	480[d,h]	27	−160	−114	0.0
γ-[MnTClPP][TCNE]	2195 m 2137 s	*f*	86	18 700	5.40	10.8	8.2	793[d]	27	−265	−189	0.1
[MnTP′P][TCNE]· 2PhMe, **4**[9]	2197 m 2133 s	*f*	90	18 500	4.90	15	13	*c*	*d*	*g*	*c*	

[a] M(5 K, 5 T); saturation not achieved at 5 T. [b] 10 Hz. [c] From d$M(H)$/dH. [d] From a fit to the Seiden expression.[16] [e] From a fit to $-T_{min}/4.2$.[19] [f] Not determinable. [g] Does not fit the Seiden expression well. [h] The observed value is too low due to solvent loss; see the text.

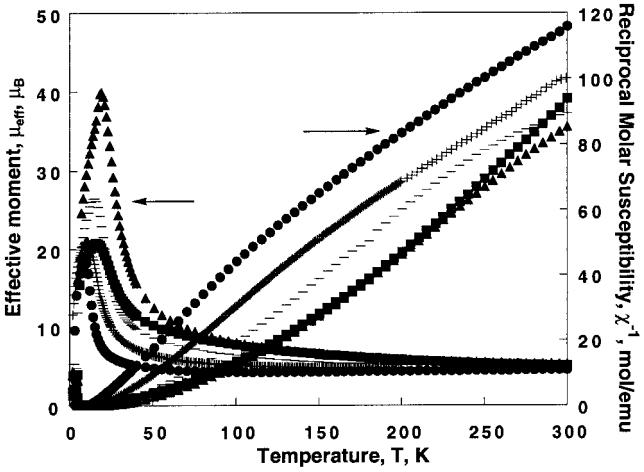

Figure 7. Reciprocal molar magnetic susceptibility, χ^{-1}, and moment, μ_{eff}, as a function of temperature (1000 Oe) for [MnTClPP][TCNE]· 2PhMe, **1** (●), α-[MnTClPP][TCNE] (+), *β*-[MnTClPP][TCNE] (■), [MnTClPP][TCNE]·$2CH_2Cl_2$, **2** (−), and *γ*-[MnTClPP][TCNE] (▲).

alternating classical ($S = 2$) and quantum ($S = {}^1/_2$) spin sites derived by Seiden[17] to solely estimate the intrachain coupling, J/k_B (k_B = Boltzmann's constant), Figure 8. At low temperatures the data deviate from the model due to the onset of interchain interactions which may be either ferromagnetic or antiferromagnetic. All compounds studied herein deviate from the Seiden prediction at lower temperatures consistent with ferromagnetic coupling as also noted for **3**[5] and **4**[10] but not $[MnOEP][C_4(CN)_6]$.[18] However, due to poor fitting of the data, quantitative fits to the Seiden function for **3**[5] and **4**[10] have not been made.

Above ∼72 K the shape of the $\chi T(T)$ for **1** can be fit to the Seiden expression (using $H = -2J\mathbf{S}_a\cdot\mathbf{S}_b$ and $g = 2$) with $J/k_B = -33$ K.[19] This fit predicts a 102 K T_{min}, which is in good agreement with the observed value of 110 K. The data for the α- and *β*-phases fit above 76 and 174 K with J/k_B's of −65 and −267 K, respectively. The 195 K T_{min} for α is in good agreement with the observed value of 192 K, while T_{min} exceeds 300 K for *β*. The Seiden fit, however, provides an estimate of 800 K for T_{min} for *β*. The Seiden fit to **2** above 40 K yields a

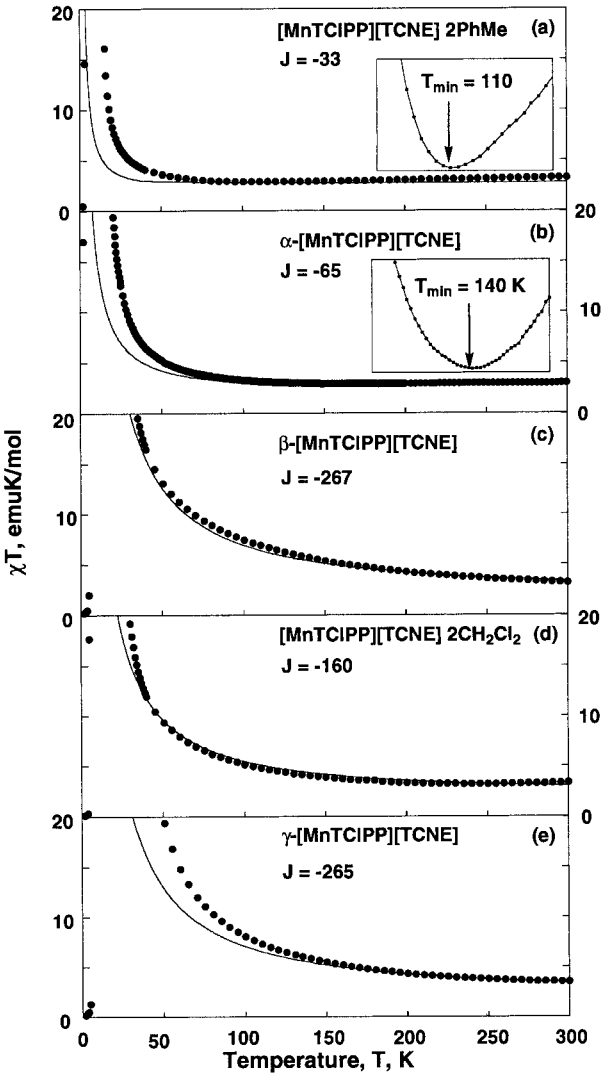

Figure 8. Fit of the $\chi T(T)$ data to the Seiden expression[16] for (a) [MnTClPP][TCNE]·2PhMe, **1**, (b) α-[MnTClPP][TCNE], (c) *β*-[MnTClPP][TCNE], (d) [MnTClPP][TCNE]·$2CH_2Cl_2$, **2**, and (e) *γ*-[MnTClPP][TCNE].

J/k_B of −160 K and a calculated $T_{min} \sim 480$ K. The observed T_{min} for **2** is 245 K, but this is probably an artifact as the sample loses solvent at higher T leading to the observation of a reduced T_{min}. Above *ca.* 170 K the *γ*-phase data can be fit to the Seiden

(17) Seiden, J. *J. Phys. Lett.* **1983**, *44*, L947.
(18) Miller, J. S.; C. Vazquez, C.; Jones, N. L.; McLean, R. S.; Epstein, A. J. *J. Mater. Chem.* **1995**, *5*, 707.
(19) The low moment for **1** leads to a displacement of the $\chi T(T)$ as calculated by the Seiden expression. To simply compare the shapes of the curves the observed $\chi T(T)$ was increased by 14%.

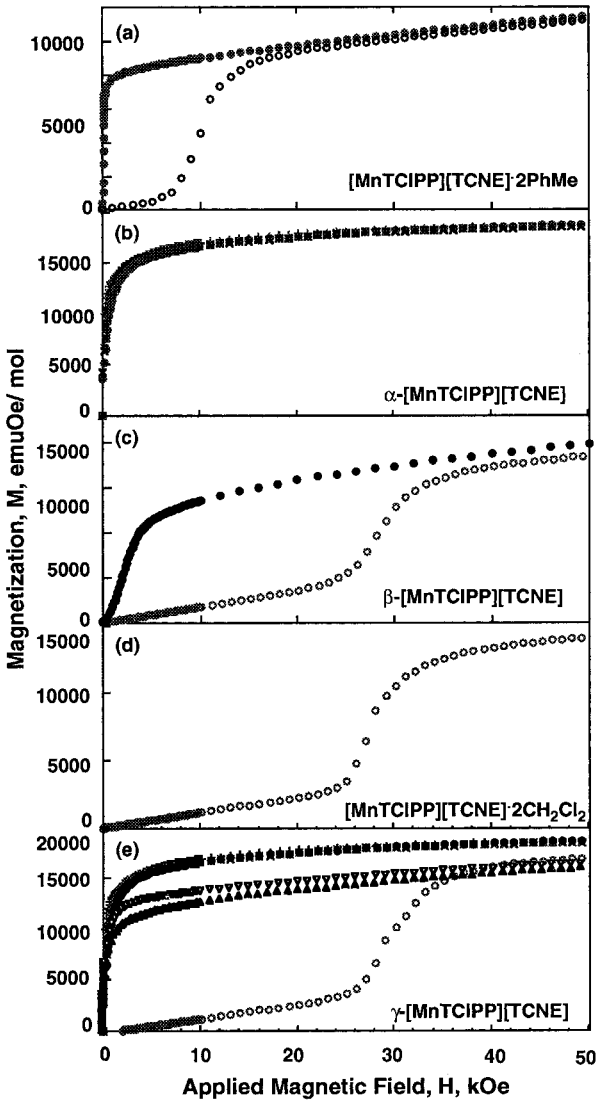

Figure 9. Field dependencies of the magnetization, $M(H)$, for (a) [MnTClPP][TCNE]·2PhMe, **1**, (b) α-[MnTClPP][TCNE], (c) β-[MnTClPP][TCNE], (d) [MnTClPP][TCNE]·$2CH_2Cl_2$, **2**, and (e) γ-[MnTClPP][TCNE] at 2 (○), 3 (+) 4, (×), 5 (●), 6 (▽), or 12 (△) K.

expression with $J/k_B = -265$ K and leads to a 793 K estimate of T_{min}. Hence, these J/k_B's and T_{min}'s are consistent with the dichloromethane solvate having stronger antiferromagnetic coupling with respect to the toluene solvate and thermal treatment enhancing the coupling as evidenced by the greater magnitudes of J/k_B as well as T_{min} as also noted for Θ' (*vide supra*).

The intrachain coupling, J/k_B, may also be approximated by the relationship $J/k_B = -T_{min}/4.2$ for $H = -2J\mathbf{S}_a.\mathbf{S}_b$.[20,21] J/k_B for **1**, α, and **2** are −26, −46, and −114 K, respectively. Using the T_{min} estimated from the Seiden expression, J/k_B is estimated to be −190 and −189 K for the β- and γ-phases, respectively. Both models give the same trend; however, the latter model gives values of J/k_B lower by $\sim 2^{1/2}/2$.

Ferrimagnetic behavior is also evident from the saturation magnetization, M_s, values, Figure 9. M_s ranges from 11 000 (**1**) to 18 700 emuOe/mol {γ-[MnTClPP][TCNE]}. These 5 K data are in accord with the expectation of antiferromagnetic coupling, *i.e.*, 16 755 emuOe/mol for $S_{Tot} = 2 - {}^1/_2$ system, which is substantially lower than the expectation for ferromagnetic coupling, *i.e.*, 27 925 emuOe/mol for $S_{Tot} = 2 + {}^1/_2$ system. The values exceeding 18 000 emuOe/mol are surprisingly high and may, in part, be a consequence of larger than expected g values.

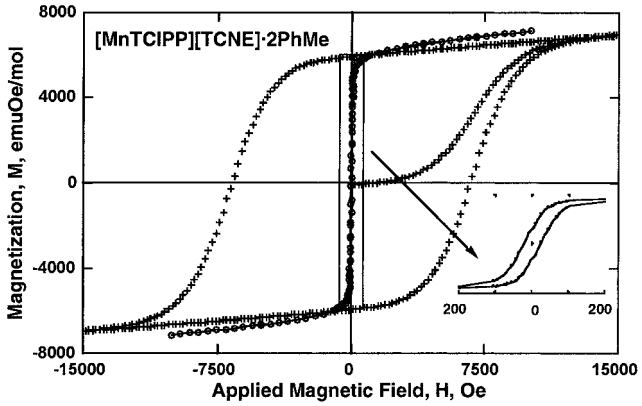

Figure 10. Hysteretic behavior for [MnTClPP][TCNE]·2PhMe, **1**, at 2 and 5 K.

The rapid rise and approach to saturation in the $M(H)$ data for α-[MnTClPP][TCNE], Figure 9, is typical for long-range ferromagnetic coupling as also evidenced by the positive Θ' values. This is also observed for the phases **1**, β, **2**, and γ at the higher temperatures studied; however, at lower temperatures a slow rise in $M(H)$ with increasing H is observed until a critical field, H_c, is reached and then a rapid rise to a high moment state occurs. This is characteristic of metamagnetic behavior. The H_c's for metamagnetic behavior are 10 kOe for **1** and 27 kOe each for the phases β, **2**, and γ, while the critical temperatures are between 2 and 5 K for **1** and **2**, ∼4 K for β-[MnTClPP][TCNE], Figure 9d, and ∼2 K for γ-[MnTClPP]-[TCNE], Figure 9e, the best studied systems. $[Fe(C_5Me_5)_2]$-[TCNQ][22] (TCNQ = 7,7,8,8-tetracyano-*p*-quinodimethane) and **3**[23] are also metamagnets. H_c for $[Fe(C_5Me_5)_2][TCNQ]$ is a much lower 1.6 kOe;[22] however, it is a comparable 24 kOe for **3**.[23] Hysteresis loops characteristic of metamagnetic behavior with a coercive field, H_{cr}, of 5.8 kOe were observed for **1** at 2 K and 25 Oe at 5 K, Figure 10. Unlike for $[Fe(C_5Me_5)_2]$-[TCNQ], the actual T_c for antiferromagnetic ordering which occurs for $H < H_c$ and as noted above is estimated to be less than 5 K cannot be more precisely identified from either $d\chi(T)/dT$ or $d\chi T(T)/dT$ plots, as maxima ascribable to these transitions are not discernible. **3** also lacks a clearly defined T_c.[23] This perhaps is a consequence of transitions to other magnetically ordered phases above this T_c which are not present for $[Fe(C_5Me_5)_2][TCNQ]$.[22]

The in-phase, real and out-of-phase, imaginary components of the complex ac susceptibility, $\chi'(T)$ and $\chi''(T)$, respectively, were determined for the phases **1**, α, β, **2**, and γ below 20 K, Figure 11. The ordering temperature, T_c, is determined from the maxima in the χ' data taken at 10 Hz and is 8.8, 6.7, 11.1, 14.1, and 11.4 K for the phases **1**, α, β, **2**, and γ, respectively. $\chi''(T, 10\ Hz)$ with maxima at 6.4, 5.8, 9.6, 8.0, and 8.2 K,

(20) Drillon, M.; Coronado, E.; Georges, R.; Gianduazzo, J. C.; Curely, J. *Phys. Rev. B* **1989**, *40*, 10992.
(21) This relationship has been obtained from a numerical model that considers the exact quantum nature of the $S = 2$ spin; hence discrepancies with the classical Sieden model reflect the limitations imposed when the $S = 2$ spin is taken as a classical spin.
(22) Candela, G. A.; Swartzendruber, L. J.; Miller, J. S.; Rice, M. J. *J. Am. Chem. Soc.* **1979**, *101*, 2755.
(23) Zhou, P.; Morin, B. G.; Epstein, A. J.; McLean, R. S.; Miller, J. S. *J. Appl. Phys.* **1993**, *73*, 6569. Brinckerhoff, W. B.; Morin, B. G.; Brandon, E. J.; Miller, J. S.; Epstein, A. J. *J. App. Phys.* **1996**, *79*, 6147.

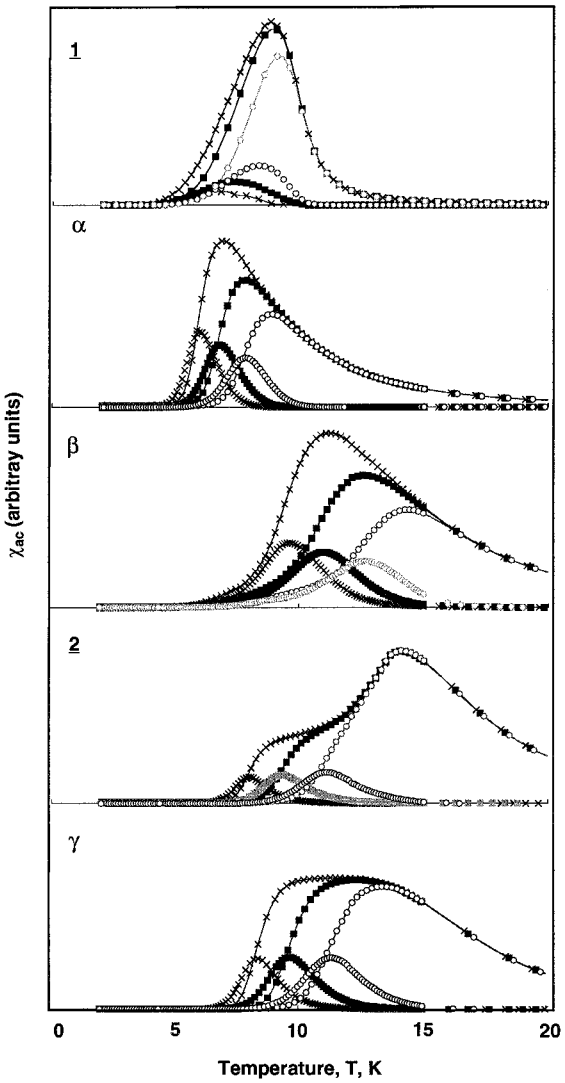

Figure 11. Temperature dependencies of the dispersive, χ' (-×-, -■-, and, -○-) and absorptive, χ'' (×, ■, and ○), components of the ac susceptibility at 10, 10^2, and 10^3 Hz, respectively, for (a) [MnTClPP][TCNE]·2PhMe, **1**, (b) α-[MnTClPP][TCNE], (c) *β*-[MnTClPP][TCNE], (d) [MnTClPP][TCNE]·$2CH_2Cl_2$, **2**, and (e) *γ*-[MnTClPP][TCNE] (H_{dc} = 0 Oe, amplitude = 1 Oe). Samples were zero-field cooled, and data were taken upon warming.

respectively, are present consistent with the presence of an uncompensated moment. As expected these values are lower than the $\chi'(T)$ counterparts. For **1**, α, *β*, and *γ* both $\chi'(T)$ and $\chi''(T)$ are frequency, *f*, dependent indicative of spin-glass behavior and/or disorder/frustration of the spin coupling.[24] The amount of disorder can be parametrized by ϕ [$\equiv \Delta T^{ac}_{max}/T^{ac}_{min}\Delta \log(f)$].[24] ϕ ranges from 0.017 (**1**) to 0.15 (α) indicating that α is the most disordered. In contrast, **2** is frequency independent ($\phi = 0$) for the peak in χ' and has the highest T_c for this family of compounds with a maximum at 14.1 K. The T_c values for **3** and **4** are 13 K. **3** as evidenced from the ϕ values has a greater amount of disorder, but ϕ for **4** has not been determined. Furthermore, **2** exhibits a second absorption at lower temperature which we attribute to the presence of the lower T_c but higher Θ′ and higher T_{min} *γ*-phase. This is a consequence of the facile ability of **2** to lose CH_2Cl_2 and concomitant difficulty in isolating solvated **2**. Thermolysis of both **1** and **2** leads to desolvated phases with more disorder.

(24) Mydosh, J. A. *Spin Glasses*; Francois and Taylor: Washington, DC, 1993.

Conclusion

The toluene and dichloromethane solvates of [MnTClPP][TCNE], each possessing a chain structure with differing intra- and interchain interactions, have been characterized. In the case of [MnTClPP][TCNE]·2PhMe, the intrachain coupling, as reflected in the observed T_{min} in $\chi T(T)$ is significantly weaker compared to the previously characterized **3** and **4** derivatives, while [MnTClPP][TCNE]·$2CH_2Cl_2$ has stronger magnetic couplings than **3**. Considering also the variations in the observed dc susceptibilities and Θ values, this suggests the degree of metal−radical coupling may be controlled by variation of the porphyrin substitution pattern. Thermal treatment of the toluene solvate results in desolvation and a change in the IR spectra, which is also manifested in a significant increase in the intrachain coupling strength as determined from dc magnetic measurements.

Acknowledgment. The authors appreciate the constructive comments and insight provided by Prof. E. Coronado (Universidad de Valencia) and Prof. A. J. Epstein, Dr. C. M. Wynn, and Mr. M. Girtu (The Ohio State University), as well as Dr. B. M. Burkhart (Hauptman-Woodward Medical Research Institute), for evaluation of structural disorder, and B. G. Dimetry (University of Utah), for time-dependent IR studies, and gratefully acknowledge the support from the U.S. Department of Energy Division of Materials Science (Grant Nos. DE-FG02-86ER45271.A000 and DE-FG03-93ER45504) and the National Science Foundation (Grant No. CHE9320478).

Supporting Information Available: Tables providing a summary of the crystallographic data, fractional coordinates and isotropic thermal parameters, anisotropic thermal parameters, bond distances and angles, and intramolecular nonbonding distances for [MnTClPP][TCNE]·2PhMe and [MnTClPP][TCNE]·$2CH_2Cl_2$ (16 pages). Ordering information is given on any current masthead page.

IC971521Z